Cancer Immunology, Immunotherapy (2023) 72:1647–1660
https://doi.org/10.1007/s00262-022-03357-4

RESEARCH

NLRP3 in tumor-associated macrophages predicts a poor prognosis and promotes tumor growth in head and neck squamous cell carcinoma

Lei Chen[1] · Shu-Cheng Wan[1] · Liang Mao[1] · Cong-Fa Huang[1] · Lin-Lin Bu[1,2] · Zhi-Jun Sun[1,2]

Received: 29 July 2022 / Accepted: 23 December 2022 / Published online: 31 December 2022

Abstract

The NOD-like receptor family pyrin domain-containing 3 (NLRP3) inflammasome plays cell- and tissue-specific roles in cancer, meaning that its activation in different tumors or cells may play different roles in tumor progression. We have previously described the tumor-promoting function of tumor-intrinsic NLRP3/IL-1β signaling in head and neck squamous cell carcinoma (HNSCC), but its role in immune cells remains unclear. In this study, we found that NLRP3 was highly expressed in tumor-associated macrophages (TAMs) in both mouse and human HNSCC, and the expression of NLRP3 was positively correlated with the density of TAMs according to immunohistochemistry, immunofluorescence, and flow cytometry analyses. Importantly, the number of NLRP3^{high} TAMs was related to worse overall survival in HNSCC patients. Knocking out NLRP3 inhibited M2-like macrophage differentiation in vitro. Moreover, the carcinogenic effect induced by 4-nitroquinoline-1-oxide was decreased in *Nlrp3*-deficient mice, which had smaller tumor sizes. Genetic depletion of NLRP3 reduced the expression of protumoral cytokines, such as IL-1β, IL-6, IL-10, and CCL2, and suppressed the accumulation of TAMs and myeloid-derived suppressor cells (MDSCs) in mouse HNSCC. Thus, activation of NLRP3 in TAMs may contribute to tumor progression and have prognostic significance in HNSCC.

Keywords NLRP3 inflammasome · Head and neck squamous cell carcinoma · Tumor-associated macrophages · Progression

Abbreviations

4NQO	4-Nitroquinoline-1-oxide
CM	Cultured medium
HNSCC	Head and neck squamous cell carcinoma
MDSCs	Myeloid-derived suppressor cells
NLRP3	NOD-like receptor family pyrin domain-containing 3
OS	Overall survival
PBMCs	Peripheral blood mononuclear cells
PDA	Pancreatic ductal adenocarcinoma
TAMs	Tumor-associated macrophages
TCGA	The cancer genome atlas
TME	Tumor microenvironment
TILs	Tumor-infiltrating lymphocytes

✉ Lin-Lin Bu
lin-lin.bu@whu.edu.cn

✉ Zhi-Jun Sun
sunzj@whu.edu.cn

[1] The State Key Laboratory Breeding Base of Basic Science of Stomatology (Hubei-MOST) & Key Laboratory of Oral Biomedicine Ministry of Education, School & Hospital of Stomatology, Wuhan University, Wuhan 430079, China

[2] Department of Oral Maxillofacial-Head Neck Oncology, School & Hospital of Stomatology, Wuhan University, Wuhan 430079, China

Introduction

Chronic inflammation is an important process in tumorigenesis and progression [1], and cancer-related inflammation has been recognized as one of the ten hallmarks of cancer [2]. The NOD-like receptor family pyrin domain-containing 3 (NLRP3) inflammasome is recognized as the most extensive sensor of harmful stimuli among innate inflammatory responses [3], which fights infection or trauma by inducing the maturation and release of interleukin (IL)-1β and IL-18, eliciting an acute inflammatory response and triggering pyroptosis [3]. Activation of the NLRP3 inflammasome plays an important role in many aspects of tumorigenesis and antitumor immunity [4]. However, its activation

in different tumor or cell types may have divergent roles in tumor progression [5, 6]. It can not only play a protumorigenic role by enhancing proliferation, metastasis and immunosuppression, but it can also play an antitumorigenic role by protecting the intestinal mucosa, activating effective antitumor immune cells, and sensitizing chemotherapy [5]. These findings highlight the complexity and diversity of NLRP3 inflammasome functions, and exploring its specific mechanisms in tumorigenesis is crucial for understanding the differences in the carcinogenesis of different tumors and developing more precise therapies.

Head and neck squamous cell carcinoma (HNSCC) is an inflammation-related heterogeneous malignancy with high metastasis and recurrence rates [7–9]. According to 2020 statistics, nearly 890,000 patients are diagnosed with HNSCC worldwide and approximately half of these patients die every year [10]. The incidence of HNSCC continues to rise, with an estimated 30% increase by 2030 [8, 11]. The treatment of HNSCC remains challenging. Despite an improved understanding of its epidemiology and pathogenesis, the 5-year survival rate of patients has been little ameliorated over the past decades [11, 12]. The NLRP3 inflammasome has a tumor-promoting role in HNSCC and is associated with tumor growth and metastasis [13] and 5-fluorouracil resistance [14]. Our previous studies have revealed that tumor-intrinsic NLRP3 signaling promotes the secretion of the cytokine IL-1β, which contributes to the formation of an inflammatory tumor microenvironment (TME) [15]. IL-1β can promote the maintenance of cancer stemness and curtail anticancer immunity by recruiting immunosuppressive cells and inducing T-cell exhaustion [15, 16]. However, the role of NLRP3 signaling in immune cells in the development and progression of HNSCC is poorly characterized.

The smoldering inflammatory TME could promote the recruitment and differentiation of TAMs, which in turn could reshape the tumor-supportive milieu through the production of mediators such as IL-1β, IL-6, and IL-10 [17, 18]. TAMs are among the most abundant immune cells of the TME and are correlated with tumor occurrence, metastasis, and immunosuppression [18]. Tumors with a high density of TAMs generally exhibit aggressive behavior and contribute to a poor prognosis, including in HNSCC [19]. Abnormally activated NLRP3 in TAMs has been reported to be a pro-tumoral signal. For instance, upregulation of the NLRP3 inflammasome has been observed in TAMs of colorectal cancer, which may contribute to the liver metastasis of tumors [20]. NLRP3/IL-1β signaling in macrophages regulates breast cancer metastasis [21]. In pancreatic ductal adenocarcinoma (PDA), NLRP3 could promote the amplification of immunosuppressive macrophages; moreover, NLRP3 signaling activation in TAMs could influence the differentiation of $CD4^+$ T cells, allowing tumor-promoting subsets to dominate, thus facilitating PDA progression [22]. Additionally, metastasis of lung cancer is also related to the activation of the NLRP3 pathway in TAMs [23]. Activation of the NLRP3 inflammasome may act as a promoter in multiple myeloma initiation and progression [24]. Despite this considerable evidence indicated that NLRP3 signal on TAMs plays a crucial role in the progression of multiple tumors, its actual function in HNSCC remains completely fuzzy. Therefore, this prompted us to investigate whether NLRP3 on TAMs plays a similar role in HNSCC.

Here, we demonstrate that in HNSCC, NLRP3 is overexpressed in TAMs and is positively correlated with TAM abundance. Patients with elevated NLRP3 expression in TAMs may have a worse prognosis. In vitro depletion of NLRP3 inhibits the polarization of M2 phenotype macrophages. In the 4NQO-induced HNSCC mouse model, we further showed that loss of NLRP3 delays tumor growth and relieves the immunosuppressed tumor state. Our data suggest that TAMs promote HNSCC tumor growth through NLRP3/IL-1β signaling.

Materials and methods

Antibodies

Immunohistochemistry and immunofluorescence: Anti-human NLRP3 (HPA012878) was obtained from Sigma-Aldrich. Anti-human CD206 (91992), anti-mouse CD206 (24595), anti-human CD163 (93498), anti-mouse F4/80 (70076), anti-human CD11b (49420) and anti-human Caspase-1(2225) were all from Cell Signaling Technology. Anti-mouse NLRP3 was obtained from Abmart (T55651). Anti-mouse IL-1β (GB11113) and anti-mouse Gr-1 (GB11229) were purchased from Servicebio. Anti-keratin K14 (GP-CK14) was from PROGEN.

Flow Cytometry: PE anti-human/mouse NLRP3 (IC7578P) was obtained from R&D Systems. PerCP-Cyanine5.5 anti-human CD14 (45-0149-42), APC anti-human CD206 (17-2069-42), PerCP-Cyanine5.5 anti-mouse F4/80 (45-4801-80), APC anti-mouse CD206 (17-2069-42), PE-Cyanine7 anti-human CD68 (25-0689-42), APC anti-mouse Ly6C (17-5932-82), PE-Cyanine7 anti-mouse Ly6G (25-9668-82) and eFluor 506 Fixable Viability Dye (65-0866-14) were from eBioscience. FITC anti-mouse CD11b (101206) was obtained from BioLegend.

Human samples

Tissue microarray. The HNSCC tissue microarray used in our study included 157 primary HNSCC, 61 oral epithelial dysplasia, and 20 normal oral mucosal samples (collected between 2011 and 2016). The pathologic diagnosis was made by two independent pathologists of the Department

of Oral Pathology, Wuhan University. In addition, 9 cases of HNSCC were lost at follow-up and were excluded from the survival analysis.

Blood and TIL. In this experiment, whole blood samples from 6 HNSCC patients were collected for the extraction of PBMCs (peripheral blood mononuclear cells). In addition, 5 freshly resected squamous cell carcinoma tissues were collected for TIL (tumor-infiltrating lymphocyte) isolation.

Mouse HNSCC samples

Tumor tissues from two different immunocompromised HNSCC mouse models were used in this experiment, including a 4NQO-induced HNSCC mouse model, and a time inducible tissue-specific *Tgfbr1*/*Pten* 2cKO (*K14*-Cre$^{ERtam\pm}$, *Tgfbr1*$^{flox/flox}$, *Pten*$^{flox/flox}$) HNSCC mouse model, which was kindly gifted by Dr. Ashok B. Kulkarni (National Institute of Dental and Craniofacial Research, USA) with material transfer agreement (NIH T-2012-1735) and United States Department of Agriculture certification (VA-12-4122R) [25]. HNSCC specimens from these models were collected in our previous study and preserved as paraffin embedded blocks.

Sample processing

PBMC. Patient and mouse PBMCs were isolated via Lymphoprep™ reagent (STEMCELL Technologies) following the manufacturer's instructions.

TIL. Freshly resected human HNSCC tissues were immediately minced into pieces and mechanically dissociated with a gentleMACS Dissociator (Miltenyi Biotec) following the manufacturer's dissociation protocol and then digested in a combined digestive solution (1 mg/ml collagenase D (Roche), 0.2 mg/ml DNase I (BIOFROXX) and 0.1 mg/ml hyaluronidase (Biosharp) in RPMI 1640 medium) for 2 h at 37 °C. Cells were filtered through 70-μm nylon cell strainers (Falcon, Fisher Scientific), and TILs were isolated with Lymphoprep™ reagent.

Lymph nodes and spleen. Tissues were ground and filtered through 70-μm nylon cell strainers using PBS with 1% FBS. Additionally, the preparation of spleen single-cell suspensions required red blood cell lysis (RBC lysis buffer, Beyotime).

Animal studies

Wild-type C57BL/6 mice were purchased from the Hubei Provincial Center for Disease Prevention and Control (Wuhan, China). *Nlrp3*$^{-/-}$ mice on the C57BL/6 background commercially available were from Shanghai Model Organisms Center (Shanghai, China). All mice were maintained in a specific pathogen-free environment at the School and Hospital of Stomatology of Wuhan University. To induce mouse HNSCC, five-week-old male *Nlrp3*$^{-/-}$ and wild-type C57BL/6 mice were given drinking water containing 50 μg/ml 4NQO (Sigma-Aldrich) for 16 weeks. Subsequently, the mice were given regular drinking water before killing. The mice were checked for oral lesions once a week after inhaled isoflurane sedation. The tumor volume was calculated as $0.5 \times \text{length} \times \text{width}^2$, and multiple tumors were summed up.

Cells

The cell lines used in this study included the human HNSCC cell line CAL27 and the human monocytic leukemia cell line THP-1 (obtained from ATCC). CAL27 cells were cultured in DMEM/high glucose medium, and THP-1 cells were cultured in RPMI 1640 medium. 10% fetal bovine serum (Gibco) and 1% penicillin/streptomycin were added to all media. To obtain the THP-1 macrophages, 1×10^6 THP-1 cells were cultured with 200 nM PMA for 48 h. For the induction of M2-like macrophages, THP-1 macrophages were incubated with CAL27 cultured medium (CM) or stimulated with recombinant human IL-4 (20 ng/ml) and IL-13 (20 ng/ml) (PeproTech) for 48 h.

Immunohistochemistry and immunofluorescence

Paraffin-embedded samples were sectioned into 4 μm sections and then deparaffinized, rehydrated, and antigen-retrieved with sodium citrate. Endogenous peroxidase was blocked with 3% hydrogen peroxide. After blocking with serum to avoid nonspecific binding, slides were incubated with the primary antibodies overnight at 4 °C. For immunohistochemistry, the sections were incubated with secondary antibodies (ZSGB-BIO) for 30 min and stained with the DAB Substrate Kit (Mxb Biotechnologies) and hematoxylin. Primary antibodies were replaced with IgG as a negative control (Supplementary Fig. 1a). To obtain the histoscore, slides were scanned by a Pannoramic MIDI scanner (3DHISTECH) and quantified by an Aperio ScanScope software (Aperio) [26]. The histoscore was normalized to 0–300. For hierarchical clustering, the histoscore of NLRP3, CD206, CD163 and CD11b from 74 HNSCC patient specimens in the tissue microarray was homogenized at -3, 0, 3, analyzed and visualized using Cluster 3.0 and Java TreeView 1.1.6. For immunofluorescence, the sections were incubated with fluorochrome-conjugated secondary antibodies (Abbkine) for 1 h in the dark. Nuclei were stained and mounted with Antifade Fluorescence Mounting Medium with DAPI (ZSGB-BIO). Images were captured under a

confocal microscope (FV1200, Olympus Life Science) and Pannoramic MIDI.

Flow cytometry

After incubation with Fc receptor blocking solution, single-cell suspensions were stained with Dead Viability dye and cell surface fluorochrome-conjugated antibodies for 1 h at 4 °C. Intracellular markers were stained with a Fixation/Permeabilization Kit (Multisciences) after staining for surface molecules as described above. Data were acquired with CytoFLEX S (Beckman Coulter), and graph drawing and data analysis were performed by using CytExpert (V2.3, Beckman Coulter) and FlowJo software (V10.0.7, TreeStar).

Immunoblotting

Cultured cells were collected and ultrasonically lysed in M-PER Protein Extraction Reagent (Thermo Fisher Scientific) with freshly added protease and phosphatase inhibitors. Quantification of protein was completed using BCA Protein Assay Kits (Beyotime). Denatured proteins were separated by 8–10% SDS-PAGE and transferred to PVDF membranes (Roche). After blocking with TBST containing 5% nonfat milk at room temperature for 1 h, the membrane was incubated with primary antibodies overnight at 4 °C and then incubated with horseradish peroxidase-conjugated secondary antibodies (Biosharp) for 1 h at room temperature. The immunoblots were visualized by a WesternBright ECL enhanced chemiluminescent substrate kit (Advansta), and the results were quantified by an Odyssey System (Li-Cor Biosciences).

Gene knockdown in THP-1

Human NLRP3 siRNA was obtained from GenePharma, and the sequences used were as follows: siNLRP3-1: 5′-GUG CAUUGAAGACAGGAAUTT-3′ (sense), 5′-AUUCCUGUC UUCAAUGCA CTT-3′ (antisense); siNLRP3-3: 5′-GUG CGUUAGAAACACUUCATT′-3′ (sense), 5′-UGAAGUG UUUCUAACGCACTT-3′ (antisense); siCtrl: 5′-UUCUCC GAACGUGUCACG UTT′-3′ (sense), 5′-ACGUGACAC GUUCGGAGAATT′-3′ (antisense). For gene knockdown, control or NLRP3 siRNA and Lipofectamine RNAiMAX reagent (Invitrogen) were diluted in Opti-MEM (Gibco) medium and mixed, and the mixture was added to THP-1 cells (2×10^5) and incubated at 37 °C for 24 h.

CCK-8

The CCK-8 assay was used to determine cell proliferation. First, CAL27 cells were seeded in a 96-well plate (5×10^3 cells per well) cultured overnight, and the medium was replaced with different components. At 0, 24, 48 and 72 h, 20 µl of CCK8 reagent (DOJINDO) was added to each well, and the plate was incubated at 37 °C for 1 h. Cell viability was assessed using a CCK-8 assay kit according to the instructions.

ELISA

Whole blood samples were collected from mice in EDTA anticoagulant tubes and centrifuged at 3000 rpm for 20 min at 4 °C, and the supernatant was used for ELISA. The supernatant of the cell culture medium was collected by centrifugation. Concentrations of IL-1β were assessed by an ELISA kit (4A Biotech, mouse, CME0015; human, CME0001) according to the manufacturer's instructions.

Luminex assay

The cytokine concentrations in the 4NQO-induced mouse tongue squamous cell carcinoma samples were measured using a Bio-Plex Pro Mouse Cytokine Grp I Panel 23-plex kit (Wayen Biotechnologies, #M6009RDPD). The Luminex liquid suspension chip detection was commissioned by Wayen Biotechnologies using a Luminex 200 system (Austin, TX, USA).

Statistical analyses

Graphs were compiled, and statistical analyses were performed with GraphPad Prism 8.0 (GraphPad). *P* values were calculated with the two-tailed unpaired *t*-test (2 groups) or one-way ANOVA tests (> 2 groups). Survival analysis was performed by two-sided log-rank (Mantel-Cox) tests. Correlations were determined by Pearson's r coefficient. Data are presented as the mean ± SD, and $P<0.05$ was considered statistically significant.

Results

NLRP3 is expressed in both tumor and stromal cells of human HNSCC

Considering that NLRP3 can be expressed in a variety of cells and may play different roles in each cell type [5], to further explore the role of NLRP3 signaling in HNSCC, this study focused on the function of NLRP3 in immune cells. By immunofluorescence detection, it was clear that NLRP3 was expressed in both tumor and stromal cells (Fig. 1a). Flow cytometry analysis showed that NLRP3 was expressed in $CD14^+$ monocytes of HNSCC TIL (Fig. 1b). We then performed IHC staining of NLRP3 using HNSCC tissue microarrays and found that NLRP3

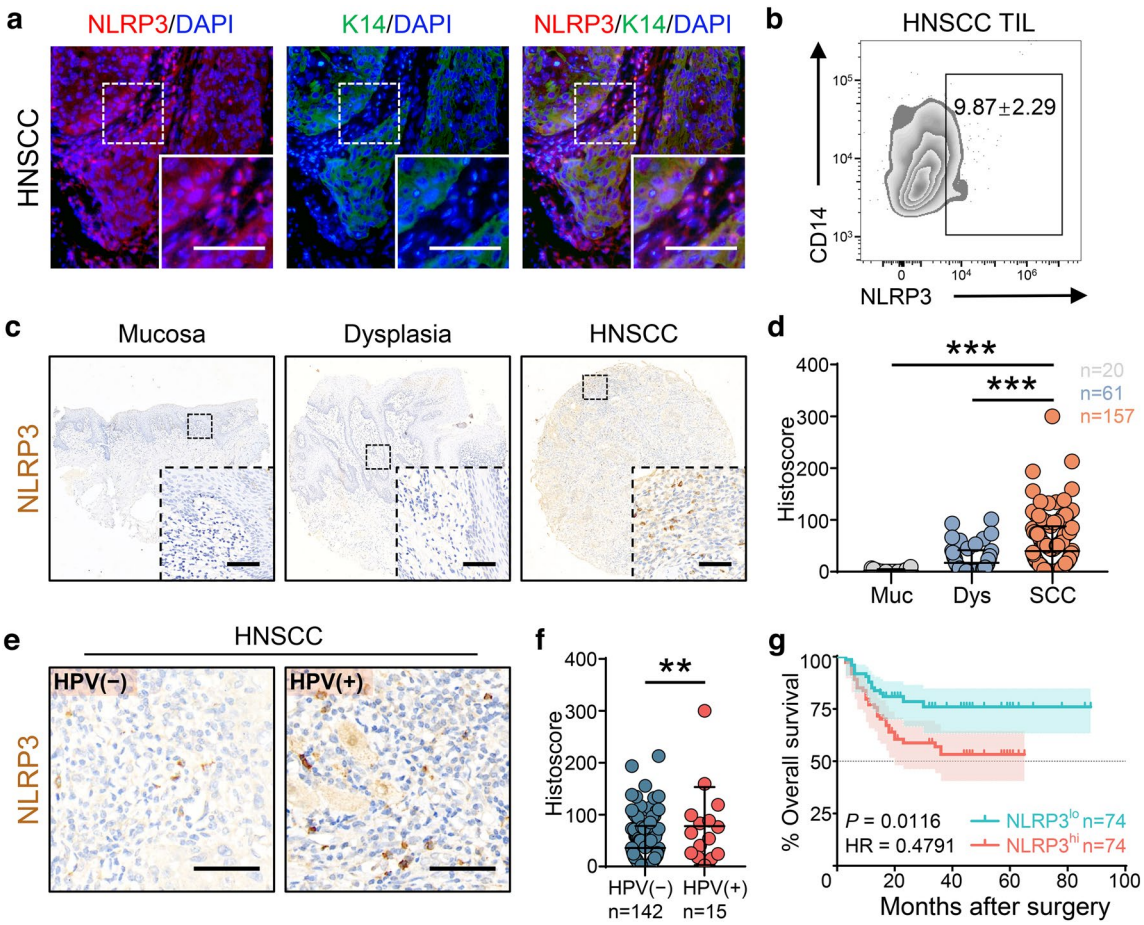

Fig. 1 NLRP3 is overexpressed in the stromal cells of human HNSCC. **a** Representative immunofluorescence images of NLRP3 (red) and CK-14 (green) in human HNSCC tissue. Bar, 50 μm. **b** Flow cytometry to detect NLRP3 expression (mean ± SD) in HNSCC TILs, and cells were gated by $CD14^{+}$. **c, d** Representative IHC images and corresponding quantification data of NLRP3 expression in oral mucosa ($n=20$), dysplasia ($n=61$) and HNSCC ($n=157$) (***, $P<0.001$). Bar, 50 μm. **e** Representative IHC staining of NLRP3 in HPV-negative ($n=142$) and HPV-positive HNSCC tissue ($n=15$) and **f** quantification analysis (**, $P<0.01$). Bar, 50 μm. **G** Kaplan–Meier analysis using overall survival (OS) of NLRP3 expression in HNSCC patients. median cut-off, $n=148$. Error bar, SD

expression in the stroma region of tumors ($n=157$) was significantly higher than that in normal mucosa ($n=20$, $P<0.001$) and dysplasia tissues ($n=61$, $P<0.001$) (Fig. 1c, d). Similarly, our previous study also found that NLRP3 was overexpressed in HNSCC tumor cells [15, 16].

We then analyzed the correlation between NLRP3 expression and clinical features and found elevated NLRP3 expression in the tumor stroma of HPV-positive patients ($P<0.01$, Fig. 1e, f). Consistently, *NLRP3* RNA expression in The Cancer Genome Atlas (TCGA) HNSCC database was found to be associated with HPV infection by using UALCAN [27] (Supplementary Fig. 1b, c). This may be the result of HPV-positive increased immune infiltration [28]. However, no significant correlation was observed between interstitial NLRP3 expression and pathological grade, TNM stage, lymph node metastasis, smoking, or alcohol consumption in our HNSCC tissue microarrays (Supplementary Table S1). Additionally, preoperative TPF chemotherapy and radiotherapy treatment significantly reduced NLRP3 expression in the tumor interstitium, and NLRP3 expression was also decreased in recurrent tumors (Supplementary Table S1).

Next, to interrogate the clinical prognostic significance of NLRP3 expression in the tumor stroma, we performed Kaplan–Meier survival analyses. The results suggested that patients with high tumor interstitial NLRP3 expression had a worse prognosis (median cut-off, $P=0.0116$, Fig. 1g; best cut-off, $P=0.0004$, Supplementary Fig. 1d). In addition, multivariate Cox analysis also indicated that high interstitial NLRP3 expression predicted reduced survival of HNSCC patients at both the median cut-off (Supplementary Table S2, $P=0.028$) and the best cut-off (Supplementary Table S3, $P=0.006$). Nevertheless, NLRP3 expression in the TCGA database was not associated with the survival of patients

with HNSCC (Supplementary Fig. 1e). This may because the TCGA data we analyzed did not calculate the expression of NLRP3 in immune cells and tumor tissues separately. Moreover, our previous study also revealed that NLRP3 in tumors does not act as a single prognostic factor [15]. Collectively, these data demonstrate that NLRP3 signaling in tumor-infiltrating immune cells may play a role in HNSCC progression.

NLRP3 overexpression in TAMs predicts poor prognosis of HNSCC patients

NLRP3 activation on immune cells that have a protumor role is mostly reported in TAMs [20–23]. To investigate whether there is a similar phenomenon in HNSCC, we performed immune cell analysis in the TCGA dataset and found that NLRP3 expression was positively correlated with both M1 and M2 phenotypes (Supplementary Fig. 2a). Unexpectedly, there was a decrease in the ratio of M1 to M2-like macrophages in patients with high NLRP3 expression (Fig. 2a, $P < 0.001$), suggesting that NLRP3 was preferentially expressed by tumor-supportive M2 phenotypes. We therefore hypothesized that NLRP3 may promote HNSCC progression through M2-type TAMs. CD206 is a recognized marker of M2-type TAMs, and immunofluorescent staining indicated that NLRP3 is preferentially expressed by TAMs (Fig. 2b). Flow cytometry analysis confirmed that NLRP3 was expressed on $CD206^+$ cells (Fig. 2c), and the expression level in HNSCC patient TILs was higher than that in PBMCs ($P < 0.01$, Fig. 2d). Furthermore, we found that the $CD206^+$ population in $CD14^+$ gated cells was increased in TILs compared to PBMCs ($P < 0.001$, Fig. 2d, Supplementary Fig. 2b), indicating that intratumoral TAMs were more abundant than in peripheral blood. Correlation analysis showed that the expression of NLRP3 in macrophages was proportional to the number of CD206-positive cells (Fig. 2e). We thus speculated that high NLRP3 expression was related to intratumoral TAM aggregation in HNSCC. To test this hypothesis, we then investigated the potential co-distribution between NLRP3 and TAMs in serial sections of HNSCC tissue microarrays by IHC and found that tumors with elevated NLRP3 expression in the stroma contained more CD163 (TAM marker) and CD206-positive cells (Fig. 2f, Supplementary Fig. 2c). In contrast, tumors with weak NLRP3 staining often had rare CD163 and CD206 expression (Fig. 2f). Pearson correlation analyses of NLRP3, CD163 and CD206 based on IHC histoscores and TCGA datasets further confirmed the positive correlation between these molecules (Fig. 2g–i).

To gain insight into the clinical significance of NLRP3 upregulation and TAM recruitment in HNSCC, survival analyses of related genes were performed. We observed that CD206 and CD163 expression did not stratify for overall survival at either protein or RNA levels (Supplementary Fig. 2d–g). However, patients with high expression of both CD206 and NLRP3 had reduced overall survival compared to patients with low expression. Moreover, among patients with high CD206 expression (median cut-off), a better survival outcome was discovered for individuals with low NLRP3 expression (Fig. 2j). In addition, survival analysis between CD163 and NLRP3 also showed consistent results (Fig. 2j). Together, the above data indicate that NLRP3 positive TAMs are associated with poor prognosis in HNSCC patients.

Upregulation of NLRP3 is associated with TAMs in mouse HNSCC

To further assess the relevance of NLRP3 signaling to TAMs in HNSCC, we examined NLRP3, CD206 and F4/80 expression in two immunocompromised spontaneous mouse HNSCC models by IHC (Fig. 3a). Consistent with the above results, Pearson correlation analysis showed that NLRP3 expression was positively correlated with CD206 and F4/80 in mouse HNSCC tissue (Fig. 3b). Likewise, an immunofluorescence assay revealed that CD206 and NLRP3, as well as F4/80 and NLRP3, were co-expressed in both *Tgfbr1*/*Pten* 2cKO and 4NQO-induced mouse HNSCC (Fig. 3c, Supplementary Fig. 3). In addition, flow cytometry analysis showed that NLRP3 could be expressed by CD206-positive macrophages in the blood of these two mouse models, and NLRP3 expression in tumor-bearing mice was higher than that in normal mice ($P < 0.001$, Fig. 1d, e). Notably, NLRP3 is absent in normal epithelial cells, while the tumor cells activate NLRP3 signaling after carcinogenesis, when NLRP3 in TAMs is already at higher levels. We therefore postulated that NLRP3 signaling in TAMs rather than squamous cells may play a leading role in tumorigenesis. Taken together, these conclusions reaffirm that NLRP3 signaling is upregulated in TAMs, which may be related to the initiation and progression of HNSCC.

TAMs promote HNSCC cell proliferation via NLRP3/IL-1β signaling

To interpret the impact of NLRP3 signaling on TAM polarization, THP-1 cells were PMA-activated into THP-1 macrophages and subsequently further differentiated into M2-like macrophages by IL-4 and IL-13 stimulation or exposure to CAL27 CM. After differentiation, the expression of NLRP3, Caspase-1 and IL-1β in M2 phenotype cells was elevated, as shown by western blotting and ELISA analyses ($P < 0.001$, Fig. 4a, b). We then used siRNA to reduce the expression of NLRP3 in THP-1 cells (Fig. 4c). Flow cytometry analysis showed that NLRP3-knockout cells had a reduced capacity to differentiate

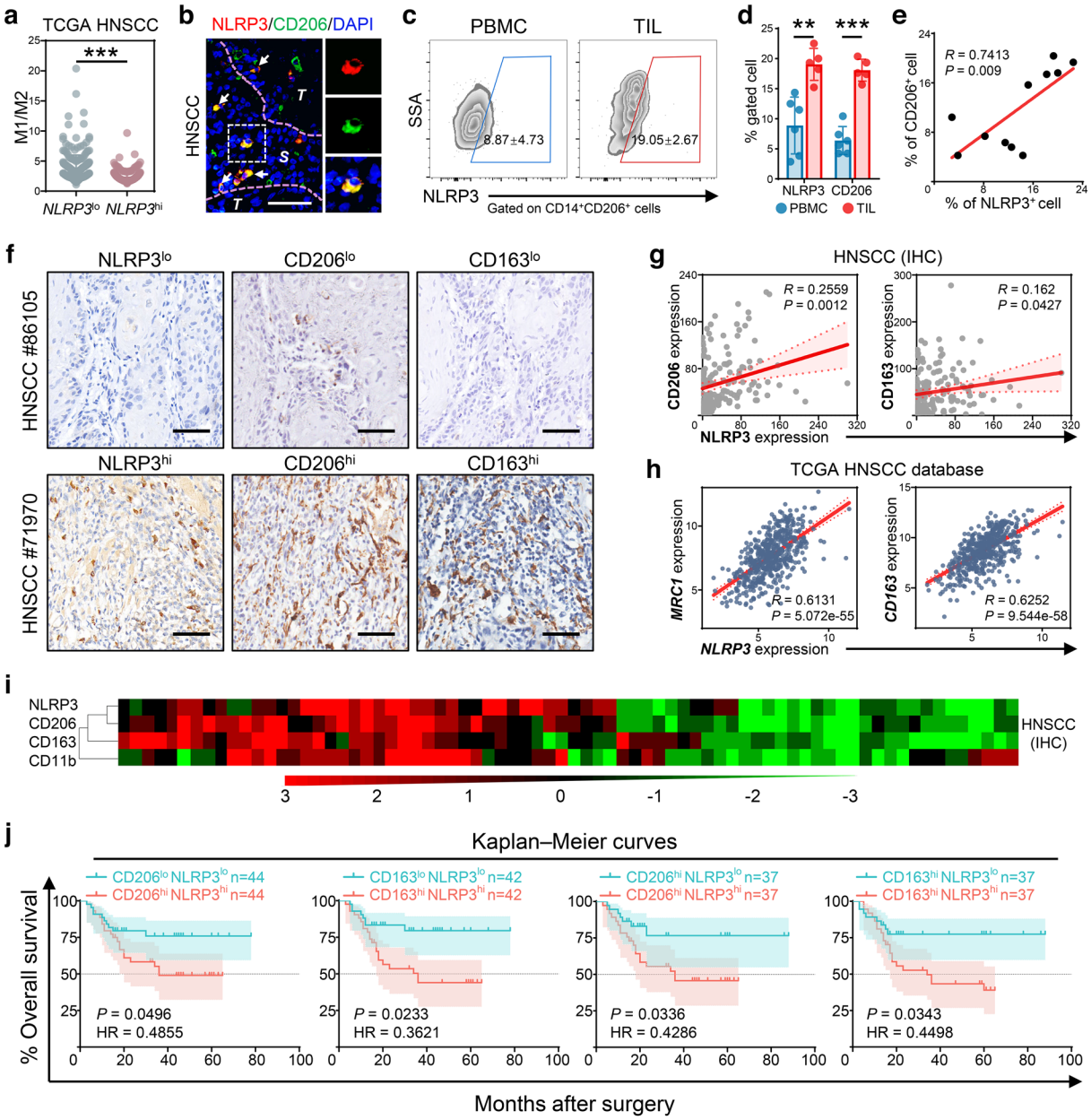

Fig. 2 Increased NLRP3 expression in TAMs predicts poor prognosis in HNSCC. **a** The ratio of M1 (*CD64*, *CD68*) and M2-like macrophage (*MRC1*, *CD163*) signatures in the low-expression ($n=259$) and high-expression NLRP3 groups ($n=259$) in the TCGA HNSCC database (***, $P<0.001$). **b** Co-immunofluorescence staining of NLRP3 (red) and CD206 (green) in human HNSCC tissue. The white arrow shows co-expressed cell (yellow). T, tumor area; S, stromal area. Bar, 50 μm. **c** Flow cytometry to detect NLRP3 expression (mean ± SD) in $CD206^+$ TAMs in human HNSCC PBMCs ($n=6$) and TILs (n=5). **d** Quantitative statistical analysis of NLRP3- and CD206-positive populations on gated cells (**, $P<0.01$; ***, $P<0.001$). **e** Correlation analysis of $CD14^+/CD206^+/NLRP3^+$ and $CD14^+/CD206^+$ cell proportions in HNSCC patient PBMC and TIL, $n=11$. **f** Representative IHC staining of NLRP3, CD206 and CD163 in human HNSCC using serial sections. Bar, 50 μm. **g** Correlation analysis between NLRP3, CD206 and CD163 protein expression in HNSCC tissue microarray using histoscore, $n=157$. **h** Correlation analysis between *NLRP3*, *MRC1* (CD206 encoding gene) and *CD163* RNA expression in the TCGA HNSCC database. unit, expression (RSEM, Log2(Val + 1)), $n=520$. **i** Hierarchical clustering plot of NLRP3, CD11b, CD206 and CD163 in HNSCC based on histoscore. $n=74$. **j** Survival curves of high NLRP3 and CD206 expression vs. low NLRP3 and CD206 expression patients; high NLRP3 and CD163 expression vs. low NLRP3 and CD163 expression patients; low NLRP3 on high CD206 expression vs. high NLRP3 on CD206 high expression patients; and low NLRP3 on high CD163 expression vs. high NLRP3 on CD163 high expression patients. Error bar, SD

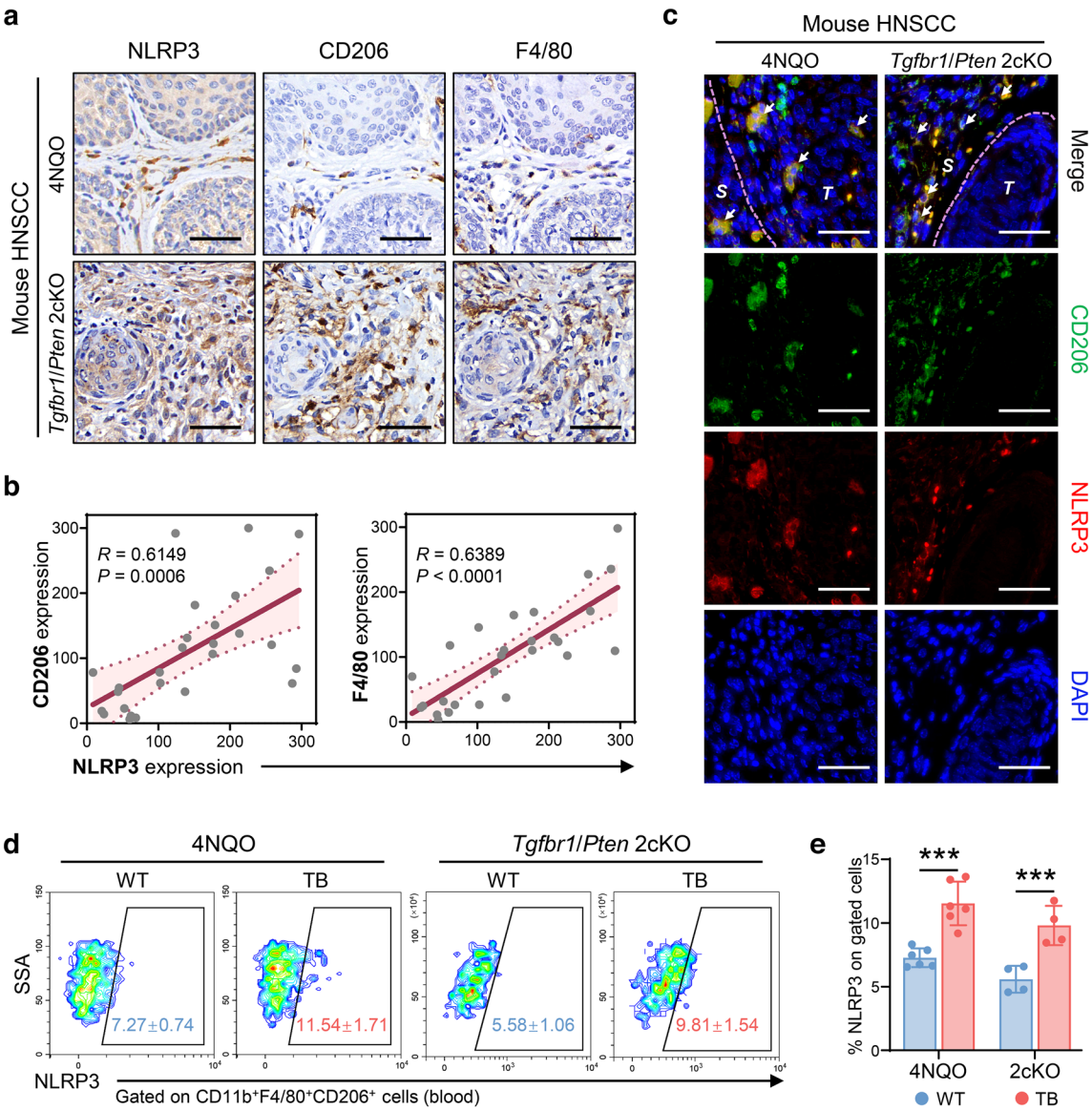

Fig. 3 NLRP3 overexpression is positively correlated with TAMs in mouse HNSCC. **a** Representative IHC images of NLRP3, CD206 and F4/80 in *Tgfbr1*/*Pten* 2cKO and 4NQO-induced mouse HNSCC tumor tissues. Bar, 50 μm. **b** Correlation analysis between NLRP3, CD206 and F4/80 expression histoscores in mouse HNSCC tissues. $n=27$. **c** Co-immunofluorescence staining of CD206 (green) and NLRP3 (red) in mouse HNSCC tissue. Bar, 50 μm. **d, e** Representative flow cytometry plots and quantification analysis showed the population change of NLRP3$^+$ TAMs in the blood of normal wild-type and tumor-bearing individuals in two mouse models ($n=6$ in 4NQO; $n=4$ in 2cKO) (***, $P<0.001$). Error bar, SD

into M2-type macrophages after CAL27 CM exposure (Fig. 4d, e). The concentration of IL-1β in the CM of the siNLRP3 group was lower than that of control group by ELISA assay ($P<0.001$, Fig. 4f). However, the proportion of NLRP3-knockdown THP-1 macrophages that differentiated into M2-like macrophages was increased after the addition of IL-1β ($P<0.001$, Fig. 4g, h). In addition, compared with THP-1 macrophages, M2-like macrophages CM had an enhanced ability to promote the proliferation of CAL27 cells, which was attenuated after depletion of NLRP3. When IL-1β was added, the proliferation ability of CAL27 cells was significantly improved ($P<0.001$, Fig. 4i). Together, these data indicate that NLRP3/IL-1β signal may be involved in the process by which TAMs promote the proliferation of HNSCC cells.

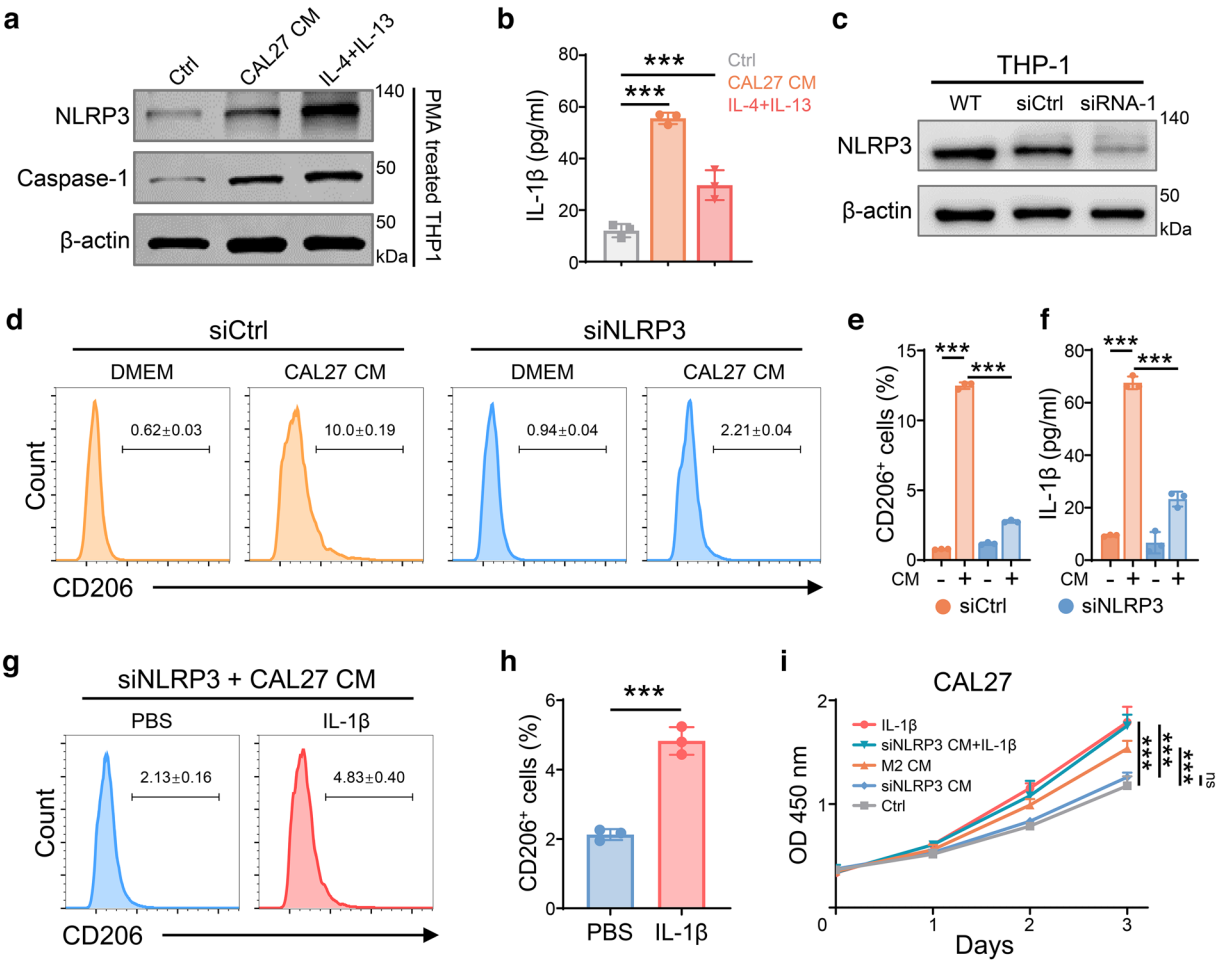

Fig. 4 Knockdown of NLRP3 in THP-1 cells inhibits M2-like macrophage polarization. **a** THP-1 cells were treated with CAL27 cultured medium (CM) or IL-4 and IL-13 after treatment with PMA; NLRP3 and Caspase-1 expression were analyzed by western blot, and **b** IL-1β amounts in the supernatant were detected by ELISA ($n=3$ per group; ***, $P<0.001$). **c** Western blotting analysis of NLRP3 expression in NLRP3-knockout or control THP-1 cells. **d, e** Flow cytometry plots and quantification analysis of CD206 in NLRP3-deficient and control THP-1 macrophages after CAL27 CM culture ($n=3$ per group; ***, $P<0.001$). **f** ELISA results of IL-1β amounts in control and siNLRP3 THP-1 macrophage cultured medium ($n=3$ per group; ***, $P<0.001$). **g, h** NLRP3-deficient THP-1 macrophages were exposed to IL-1β (20 ng/ml) for 48 h after CAL27 CM treatment, and CD206 was analyzed by flow cytometry ($n=3$ per group; ***, $P<0.001$). **i** Growth curves of CAL27 cells in different groups as measured by a CCK-8 assay ($n=3$ per group; ***, $P<0.001$). Error bar, SD

Loss of NLRP3 results in delayed development of 4NQO-induced HNSCC

The carcinogen 4NQO mimics the carcinogenic effects of tobacco consumption (Fig. 5a), and it has been extensively used to study HNSCC progression and prevention. Mice received 50 μg/mL 4NQO in the drinking water for 16 consecutive weeks, followed by normal drinking water, and oral lesions were monitored until 24 weeks (Fig. 5b). Oral neoplasia was observed in both groups at the end of the experiment (Fig. 5c, d). Nevertheless, deletion of the NLRP3 gene did not reduce tumors incidence (Fig. 5e). At 24 weeks, the oral lesions in both groups were HNSCC and a small amount of dysplasia (Fig. 5f). We found that the tumor volume of the *Nlrp3*$^{-/-}$ mice (n = 7) was smaller than that of the control group ($n=8$, $P<0.05$) (Fig. 5g, h). However, there was no significant difference in tumor number ($P=0.09$, Fig. 5i). Additionally, the weight loss in *Nlrp3*$^{-/-}$ tumor-bearing mice was milder than that in the control group. ($P<0.05$; $P<0.001$, Fig. 5j). Collectively, these findings suggest that NLRP3 knockdown could delay the growth rate of 4NQO-induced oral carcinoma and that NLRP3 may be involved in the development of HNSCC.

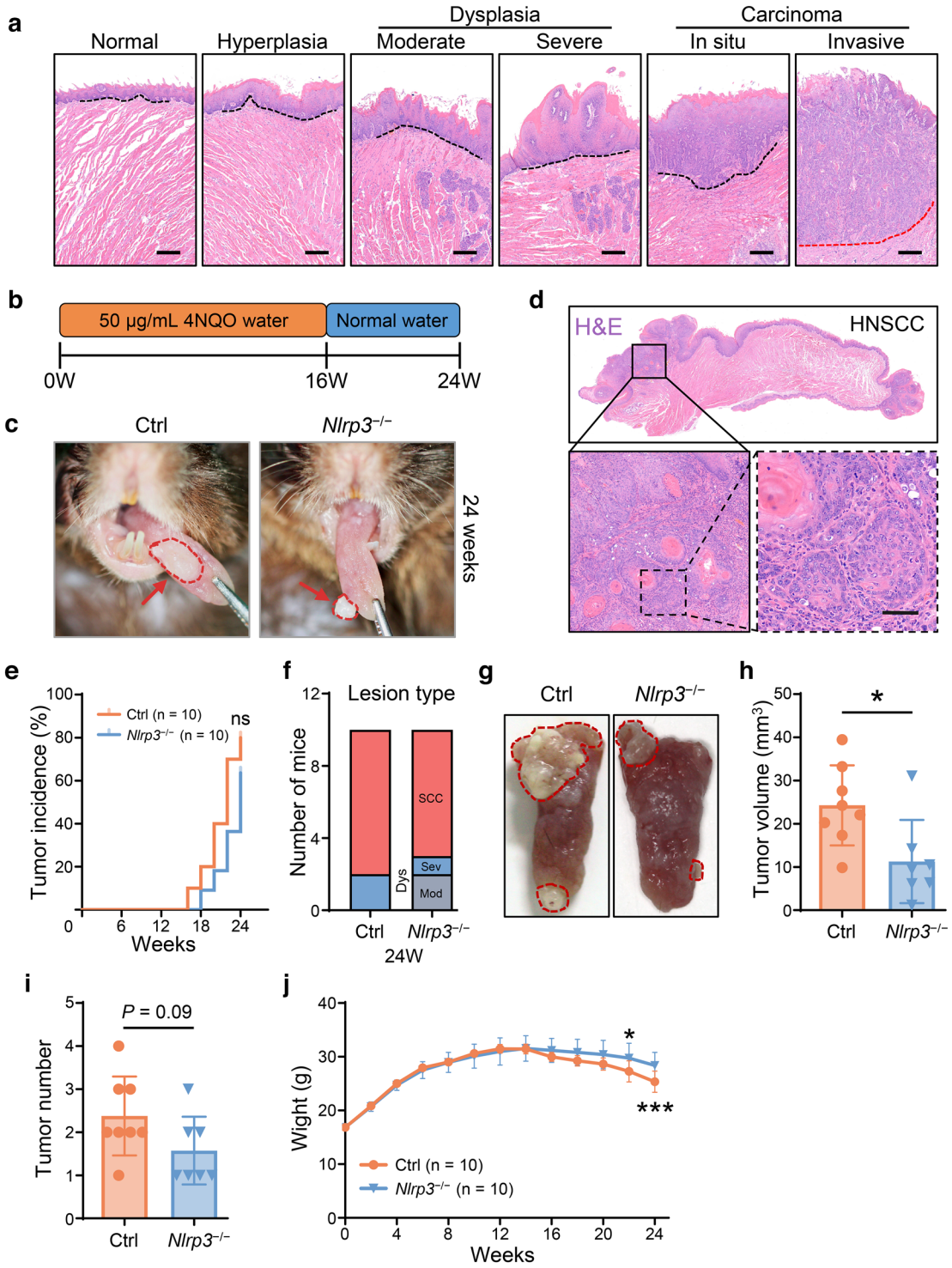

Fig. 5 Induction of HNSCC in *Nlrp3*-deficient mice by 4NQO. **a** Haematoxylin and eosin (H&E) staining showed the pathological changes in mouse tongues after 4NQO exposure. The dotted line indicates the epithelial basement membrane. Bar, 200 μm. **b** Schematic of the 4NQO tumorigenesis protocol. **c** Representative pictures of oral lesions in control and *Nlrp3*$^{-/-}$ mice at 24 weeks. **d** Representative H&E histological sections of 4NQO induced HNSCC. Bar, 50 μm. **e** Tumor incidence in the *Nlrp3*$^{-/-}$ ($n=10$) and control ($n=10$) groups. ns, no significant difference. **f** The proportion of oral lesion types in the two groups at week 24. **g** Representative image of tongue SCC in the two groups of mice. The red dotted circle denotes the lesion area. **h** Quantitative analysis of tumor size and **i** number in the *Nlrp3*$^{-/-}$ ($n=7$) and control groups ($n=8$) at the experimental endpoint. *, $P<0.05$. **j** The body weights of 4NQO-treated control and *Nlrp3*$^{-/-}$ mice from the beginning to the end of this experiment. *, $P<0.05$; ***, $P<0.001$. Error bar, SD

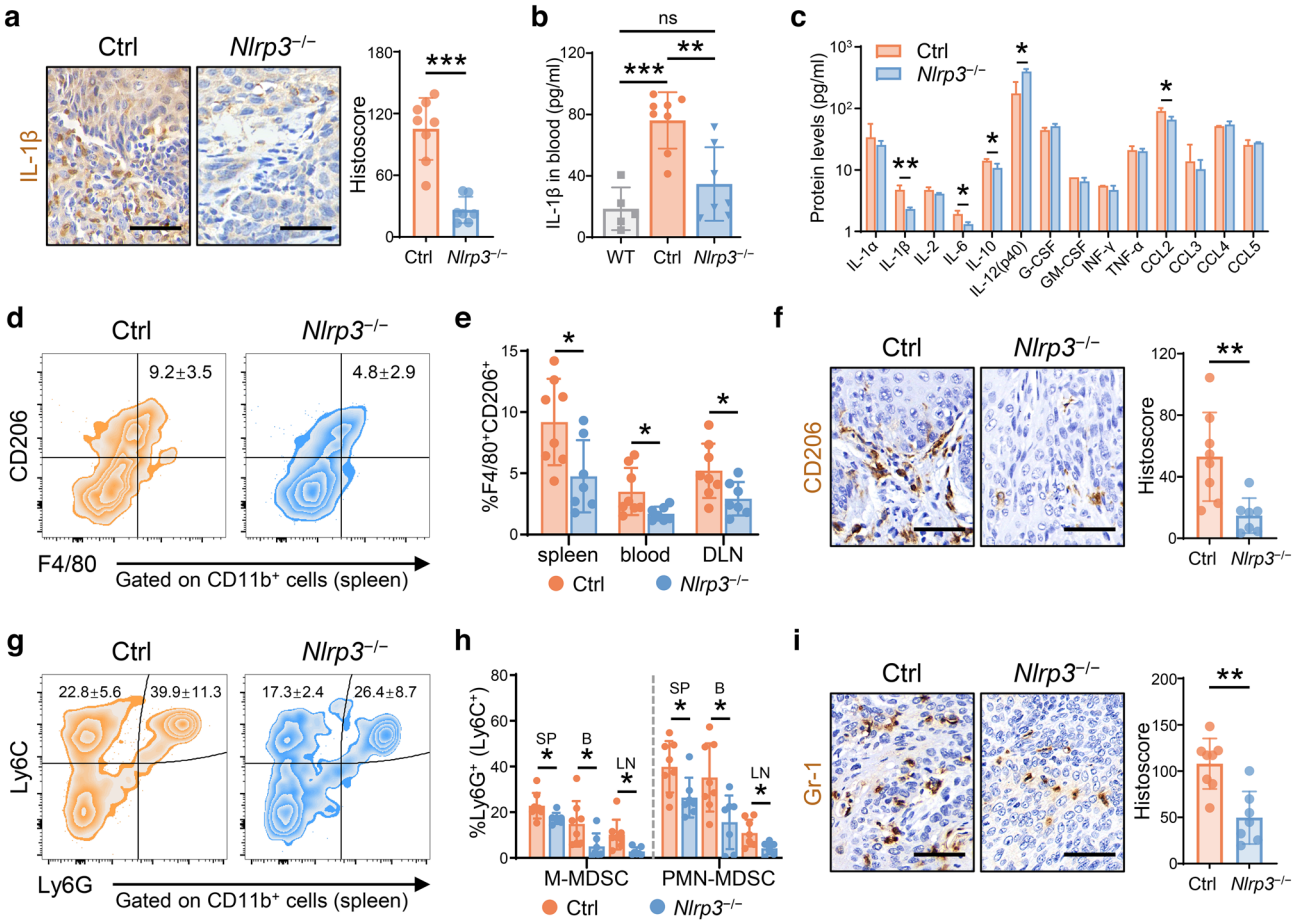

Fig. 6 NLRP3 deficiency reduced the proportion of TAMs and MDSCs. **a** Representative IHC images and quantification of IL-1β in tumor tissues from the two groups of mice. ***, $P<0.001$, Bar, 50 μm. **b** ELISA results of IL-1β amounts in the blood of normal WT ($n=5$), 4NQO-treated control ($n=8$) and *Nlrp3*$^{-/-}$ ($n=7$) tumor burden mice. **, $P<0.01$; ***, $P<0.001$; ns, no significant difference. **c** The Luminex liquid suspension chip analysis result. *, $P<0.05$; **, $P<0.01$, three mice in each group. **d** Flow cytometry to detect the percentage of CD11b$^+$/F4/80$^+$/CD206$^+$ TAMs in the spleen of the two groups and **e** quantitative statistical analysis. *, $P<0.05$. **f** Representative IHC images and quantification of CD206 in control and *Nlrp3*$^{-/-}$ mouse HNSCC tissues. **, $P<0.01$, Bar, 50 μm. **g** Flow cytometry to detect the percentage of M-MDSCs and PMN-MDSCs in the spleen of the two groups and **h** quantitative statistical analysis. *, $P<0.05$. **i** Representative IHC images and quantification of Gr-1 in control and *Nlrp3*$^{-/-}$ mouse HNSCC tissues. **, $P<0.01$, Bar, 50 μm

The immunosuppressed tumor status was alleviated in *Nlrp3*$^{-/-}$ mice

IHC staining showed that genetic ablation of NLRP3 reduced IL-1β amounts in the tumor tissue (Fig. 6a). ELISA results showed that the IL-1β concentration in the blood of tumor-bearing mice ($n=8$) was increased compared with that of normal mice ($n=5$, $P<0.001$), while NLRP3 depletion decreased the amount of IL-1β (Fig. 6b, $n=7$, $P<0.01$). *NLRP3* and *IL1B* RNA are associated with multiple cytokines in the TCGA HNSCC cohort (Supplementary Fig. 4a); thus, a Luminex suspension chip was used to detect the differential expression of common chemotactic and inflammatory cytokines in tumor tissues. We found that the expression of the protumor cytokines IL-1β, IL-6, and IL-10 in the *Nlrp3*$^{-/-}$ group was decreased compared to that in the control group (Fig. 6c), while the antitumor cytokine IL-12 was increased (Fig. 6c, $P<0.05$). Moreover, the chemokine CCL2 has been reported to promote TAM recruitment, immunosuppression, and tumor progression [29], and here, we found that NLRP3 silencing reduced its expression (Fig. 6c, $P<0.05$). To validate the effect of NLRP3 deletion on the accumulation of TAMs, flow cytometry analysis was performed. The results showed that CD11b$^+$/F4/80$^+$/CD206$^+$ cells were decreased in the blood, spleen and draining lymph nodes of NLRP3 knockout mice ($P<0.05$, Fig. 6d, e, Supplementary Fig. 4b, c). Immunostaining showed that the number of CD206 positive cells was decreased in *Nlrp3*$^{-/-}$ mouse tumor tissue (Fig. 6f). In addition, activation of the NLRP3 inflammasome can promote the recruitment of MDSCs, which, along with TAMs, play a critical role in building an immunosuppressive TME [30, 31]. In line with the results of these studies, we found that NLRP3 deletion also

reduced MDSC aggregation in mouse HNSCC (Fig. 6g–i). In summary, the current data suggest that inhibition of NLRP3/IL-1β signaling may improve the tumor immunosuppression state in HNSCC.

Discussion

Inflammation and immunity are identified as determinants of tumorigenesis [1]. Studies have demonstrated the promoting role of chronic inflammation in the occurrence and development of cancers. Pro-cancer inflammation is thought to allow cancer cells to evade immune surveillance while promoting genetic instability, survival, and progression [32]. The NLRP3 inflammasome is a danger sensor of the immune system that induces the maturation and release of the inflammatory mediator IL-1β and IL-18, and promotes cell pyroptosis, thereby effectively driving the immune response [3]. Cancer cells are able to hijack this normal physiological sensing mechanism to promote tumor progression. Aberrant activation of the NLRP3 inflammasome was observed in 15 types of cancer [33], resulting in chronic inflammation involved in multiple stages of tumor development [4–6]. However, the role of NLRP3 in carcinogenesis is considered to be contradictory and context-dependent [5, 34]. For example, IL-18 maintains colonic epithelial homeostasis, plays a protective role in colitis-associated colon cancer [35], and enhances the killing activity of NK cells against liver metastases of colon cancer cells [36]. Whereas IL-1β has a diametrically opposite effect; it suppresses tumor immune responses in breast and gastric cancers [37] and attenuates the antitumor effect of DC vaccines by recruiting MDSCs to the TME [30]. In addition, NLRP3 signaling activated in different cells also has disparate roles in cancers. Tumor-intrinsic NLRP3 mostly plays a tumor-promoting role [31, 38, 39]. Myeloid cells are the primary source of IL-1β produced by the NLRP3 inflammasome, but NLRP3 plays a different role in these cells. This is a protumoral signal in immunosuppressive TAMs [20–24] and MDSCs [40]. However, the activation of NLRP3 in DCs may enhance the efficacy of chemotherapy to suppress tumor growth [41]. Nonetheless, the NLRP3 inflammasome remains an attractive target, and its potential in the field of immunotherapy is gradually emerging [42–44]. Our previous works suggest that abnormal activation of NLRP3 signaling in cancer cells may promote HNSCC progression and immune escape [15, 16]. However, current studies on the role of NLRP3 inflammasome in HNSCC are inadequate, focusing mainly on tumor-intrinsic function, while its role in immune cells of the HNSCC TME remains puzzling. Notably, this is the first report to demonstrate that NLRP3 signaling on TAMs promotes HNSCC progression and is an independent predictor of poor prognosis.

As an important component of the TME, TAMs are associated with poor prognosis, tumor progression, metastasis and chemotherapy resistance in most cancers [18]. TAMs are highly plastic and in a dynamic and continuous state of the classically activated M1-like and alternatively activated M2-like types [45]. There is increasing evidence that NLRP3 signaling in TAMs promotes tumor progression and metastasis [20–24]. Consistently, we found a positive correlation between NLRP3 and M2 TAM-related molecules in both human and mouse HNSCC. Furthermore, the M1/M2 ratio was decreased in individuals with high NLRP3 expression from the TCGA HNSCC cohort, suggesting that NLRP3 may promote M2-type macrophage differentiation in HNSCC. Unexpectedly, another finding in the current work is that high NLRP3 expression in $CD206^+$ or $CD163^+$ macrophages was correlated with poorer overall survival in HNSCC patients. Moreover, induction of THP-1 macrophages into M2-like macrophages was accompanied by obvious up-regulation of NLRP3. After NLRP3 depletion, the process of M2 phenotype polarization was inhibited, and the proliferation capacity of cocultured CAL27 cells was also suppressed. Nevertheless, this inhibition was subsequently alleviated by IL-1β. These results indicate the role of NLRP3/IL-1β signal in the proliferation of HNSCC promoted by M2-type TAMs.

The 4NQO mouse model reflects the characteristic carcinogenic process and clinical features of human HNSCC [46, 47]. We observed a moderate but significant delay in tumor development in NLRP3 deficient mice compared to the control group. IL-1β was elevated after SCC formation, while NLRP3 deletion diminished IL-1β amounts. The Luminex chip results showed that IL-1β, IL-6, and IL-10, which promote tumor immunosuppression, were reduced, while the immune stimulator cytokine IL-12 was increased after NLRP3 knockdown. CCL2 is associated with TAM recruitment and immune evasion, NLRP3 deletion also reduced its expression in tumors. Furthermore, the flow cytometry and IHC results also showed a decrease in TAMs and MDSCs after the loss of the NLRP3 gene. These results indicate a remission of the immunosuppressed TME in *Nlrp3*$^{-/-}$ mice. Regrettably, we were unable to determine whether the immune-improving effect was caused by TAMs alone or the combined effect of NLRP3 inhibition on several cells. Studies have found that Caspase-1 in MDSCs can promote the proliferation of HNSCC [48]. Although we have emphasized the role of NLRP3 in TAMs in this work, its function in other immune cells remains to be explored. Furthermore, other components of NLRP3 inflammasome, ASC and Caspase-1, were also found to be overexpressed on TAMs and involved in tumor progression [20, 23, 24], highlighting the complexity of NLRP3 inflammasome. Further efforts are required to completely elucidate the complex roles of the individual components of inflammasome

in HNSCC progression using a mouse model of tissue- and cell-specific conditional deletion.

In summary, our study highlights the role of NLRP3/IL-1β signaling in HNSCC progression. Aberrant activation of NLRP3 in TAMs is associated with poor prognosis in HNSCC patients. NLRP3 depletion inhibited the polarization of M2-like macrophages in vitro, thus reducing the role of macrophages in promoting the proliferation of tumor cells. In the 4NQO induced HNSCC mouse model, the absence of NLRP3 improved the immunosuppressed TME. Given the diversity of NLRP3 functions, more efforts are needed to reveal the unknown mechanisms of this attractive target in HNSCC.

Supplementary Information The online version contains supplementary material available at https://doi.org/10.1007/s00262-022-03357-4.

Acknowledgements Thanks to Shuyan Liang and Juan Zhang from Wuhan Biobank Co.,Ltd for their excellent technical assistance on flow cytometry.

Author contributions CL, SZJ and BLL conceptualized the study. CL, WSC and ML developed methodology. CL, WSC and ML performed the experiments. CL and HCF analyzed data. CL, SZJ and BLL wrote the manuscript. All authors contributed to the article and approved the submitted version.

Funding This work was supported by National Natural Science Foundation of China (82103670, 81972548, 82072996, 81874131), Fundamental Research Funds for the Central Universities (2042021kf0173).

Declarations

Conflict of interest The authors declare no potential conflicts of interest.

Consent for publication All participants who provided a specimen (peripheral blood or surgically resected tumor tissues) signed informed consent under an approved institutional guideline and agreed to use the samples for research and publication.

Ethical approval All animal studies were approved by the Institutional Animal Care and Use Committees at the School and Hospital of Stomatology of Wuhan University (S07918040F and S07922050F). All the human samples were collected from the School and Hospital of Stomatology, Wuhan University, and all experiments were approved by the Medical Ethics Committee (2014LUNSHENZI06, 2016LUNSHENZI62 and 2019LUNSHENZIA24).

References

1. Taniguchi K, Karin M (2018) NF-κB, inflammation, immunity and cancer: coming of age. Nat Rev Immunol 18:309–324. https://doi.org/10.1038/nri.2017.142
2. Hanahan D (2022) Hallmarks of cancer: new dimensions. Cancer Discov 12:31–46. https://doi.org/10.1158/2159-8290.CD-21-1059
3. Swanson KV, Deng M, Ting JPY (2019) The NLRP3 inflammasome: molecular activation and regulation to therapeutics. Nat Rev Immunol 44:1229–1245. https://doi.org/10.1038/s41577-019-0165-0
4. Moossavi M, Parsamanesh N, Bahrami A, Atkin SL, Sahebkar A (2018) Role of the NLRP3 inflammasome in cancer. Mol Cancer 17:158. https://doi.org/10.1186/s12943-018-0900-3
5. Karki R, Kanneganti TD (2019) Diverging inflammasome signals in tumorigenesis and potential targeting. Nat Rev Cancer 19:197–214. https://doi.org/10.1038/s41568-019-0123-y
6. Sharma BR, Kanneganti TD (2021) NLRP3 inflammasome in cancer and metabolic diseases. Nat Immunol 22:550–559. https://doi.org/10.1038/s41590-021-00886-5
7. Ferris RL (2015) Immunology and immunotherapy of head and neck cancer. J Clin Oncol 33:3293–3304. https://doi.org/10.1200/JCO.2015.61.1509
8. Johnson DE, Burtness B, Leemans CR et al (2020) Head and neck squamous cell carcinoma. Nat Rev Dis Primers 6:92. https://doi.org/10.1038/s41572-020-00224-3
9. Bonomi M, Patsias A, Posner M, Sikora A (2014) The role of inflammation in head and neck cancer. Adv Exp Med Biol 816:107–127. https://doi.org/10.1007/978-3-0348-0837-8_5
10. Sung H, Ferlay J, Siegel RL et al (2021) Global cancer statistics 2020: GLOBOCAN estimates of incidence and mortality worldwide for 36 cancers in 185 countries. CA Cancer J Clin 71:209–249. https://doi.org/10.3322/caac.21660
11. Bray F, Ferlay J, Soerjomataram I et al (2018) Global cancer statistics 2018: GLOBOCAN estimates of incidence and mortality worldwide for 36 cancers in 185 countries. CA Cancer J Clin 68:394–424. https://doi.org/10.3322/caac.21492
12. Cramer JD, Burtness B, Le QT, Ferris RL (2019) The changing therapeutic landscape of head and neck cancer. Nat Rev Clin Oncol 16:669–683. https://doi.org/10.1038/s41571-019-0227-z
13. Wang H, Luo QQ, Feng XD et al (2018) NLRP3 promotes tumor growth and metastasis in human oral squamous cell carcinoma. BMC Cancer 18:500. https://doi.org/10.1186/s12885-018-4403-9
14. Feng XD, Luo QQ, Han Z et al (2017) The role of NLRP3 inflammasome in 5-fluorouracil resistance of oral squamous cell carcinoma. J Exp Clin Cancer Res 36:81. https://doi.org/10.1186/s13046-017-0553-x
15. Huang CF, Chen L, Li YC et al (2017) NLRP3 inflammasome activation promotes inflammation-induced carcinogenesis in head and neck squamous cell carcinoma. J Exp Clin Cancer Res 36:116. https://doi.org/10.1186/s13046-017-0589-y
16. Chen L, Huang CF, Li YC et al (2018) Blockage of the NLRP3 inflammasome by MCC950 improves anti-tumor immune responses in head and neck squamous cell carcinoma. Cell Mol Life Sci 75:2045–2058. https://doi.org/10.1007/s00018-017-2720-9
17. Xiang X, Wang J, Lu D, Xu X (2021) Targeting tumor-associated macrophages to synergize tumor immunotherapy. Signal Transduct Target Ther 6:75. https://doi.org/10.1038/s41392-021-00484-9
18. Pathria P, Louis TL, Varner JA (2019) Targeting tumor-associated macrophages in cancer. Trends Immunol 40:310–327. https://doi.org/10.1016/j.it.2019.02.003
19. Evrard D, Szturz P, Tijeras-Raballand A et al (2019) Macrophages in the microenvironment of head and neck cancer: potential targets for cancer therapy. Oral Oncol 88:29–38. https://doi.org/10.1016/j.oraloncology.2018.10.040
20. Deng QT, Geng Y, Zhao LY et al (2019) NLRP3 inflammasomes in macrophages drive colorectal cancer metastasis to the liver. Cancer Lett 442:21–30. https://doi.org/10.1016/j.canlet.2018.10.030
21. Weichand B, Popp R, Dziumbla S et al (2017) S1PR1 on tumor-associated macrophages promotes lymphangiogenesis and

metastasis via NLRP3/IL-1β. J Exp Med 214:2695–2713. https://doi.org/10.1084/jem.20160392
22. Daley D, Mani VR, Mohan N et al (2017) NLRP3 signaling drives macrophage-induced adaptive immune suppression in pancreatic carcinoma. J Exp Med 214:1711–1724. https://doi.org/10.1084/jem.20161707
23. Liang MM, Chen XW, Wang LJ et al (2020) Cancer-derived exosomal TRIM59 regulates macrophage NLRP3 inflammasome activation to promote lung cancer progression. J Exp Clin Cancer Res 39:176. https://doi.org/10.1186/s13046-020-01688-7
24. Hofbauer D, Mougiakakos D, Broggini L et al (2021) β2-microglobulin triggers NLRP3 inflammasome activation in tumor-associated macrophages to promote multiple myeloma progression. Immunity 54:1772–1787. https://doi.org/10.1016/j.immuni.2021.07.002
25. Bian Y, Hall B, Sun ZJ et al (2012) Loss of TGF-β signaling and PTEN promotes head and neck squamous cell carcinoma through cellular senescence evasion and cancer-related inflammation. Oncogene 31:3322–3332. https://doi.org/10.1038/onc.2011.494
26. Chen L, Yang QC, Li YC et al (2020) Targeting CMTM6 suppresses stem cell-like properties and enhances antitumor immunity in head and neck squamous cell carcinoma. Cancer Immunol Res 8:179–191. https://doi.org/10.1158/2326-6066.CIR-19-0394
27. Chandrashekar DS, Bashel B, Balasubramanya SAH et al (2017) UALCAN: a portal for facilitating tumor subgroup gene expression and survival analyses. Neoplasia 19:649–658. https://doi.org/10.1016/j.neo.2017.05.002
28. Ruffin AT, Li H, Vujanovic L et al (2022) Improving head and neck cancer therapies by immunomodulation of the tumour microenvironment. Nat Rev Cancer. https://doi.org/10.1038/s41568-022-00531-9
29. Yang H, Zhang QN, Xu M et al (2020) CCL2-CCR2 axis recruits tumor associated macrophages to induce immune evasion through PD-1 signaling in esophageal carcinogenesis. Mol Cancer 19:41. https://doi.org/10.1186/s12943-020-01165-x
30. Van Deventer HW, Burgents JE, Wu QP et al (2011) The inflammasome component Nlrp3 impairs antitumor vaccine by enhancing the accumulation of tumor-associated myeloid-derived suppressor cells. Cancer Res 70:10161–10169. https://doi.org/10.1158/0008-5472.CAN-10-1921
31. Tengesdal IW, Menon DR, Osborne DG et al (2021) Targeting tumor-derived NLRP3 reduces melanoma progression by limiting MDSCs expansion. Proc Natl Acad Sci USA 118:e2000915118. https://doi.org/10.1073/pnas.2000915118
32. Greten FR, Grivennikov SI (2019) Inflammation and cancer: triggers, mechanisms, and consequences. Immunity 51:27–41. https://doi.org/10.1016/j.immuni.2019.06.025
33. Ju MY, Bi J, Wei Q et al (2021) Pan-cancer analysis of NLRP3 inflammasome with potential implications in prognosis and immunotherapy in human cancer. Brief Bioinform 22:bbaa345. https://doi.org/10.1093/bib/bbaa345
34. Hamarsheh S, Zeiser R (2020) NLRP3 inflammasome activation in cancer: a double-edged sword. Front Immunol 11:1444. https://doi.org/10.3389/fimmu.2020.01444
35. Zaki MH, Vogel P, Body-Malapel M, Lamkanfi M, Kanneganti TD (2010) IL-18 production downstream of the Nlrp3 inflammasome confers protection against colorectal tumor formation. J Immunol 185:4912–4920. https://doi.org/10.4049/jimmunol.1002046
36. Dupaul-Chicoine J, Arabzadeh A, Dagenais M et al (2015) The Nlrp3 inflammasome suppresses colorectal cancer metastatic growth in the liver by promoting natural killer cell tumoricidal activity. Immunity 43:751–763. https://doi.org/10.1016/j.immuni.2015.08.013
37. Tu S, Bhagat G, Cui G et al (2008) Overexpression of interleukin-1beta induces gastric inflammation and cancer and mobilizes myeloid-derived suppressor cells in mice. Cancer Cell 14:408–419. https://doi.org/10.1016/j.ccr.2008.10.011
38. Das S, Shapiro B, Vucic EA, Vogt S, Bar-Sagi D (2020) Tumor cell-derived IL-1β promotes desmoplasia and immune suppression in pancreatic cancer. Cancer Res 80:1088–1101. https://doi.org/10.1158/0008-5472.CAN-19-2080
39. Theivanthiran B, Evans KS, Devito NC et al (2020) A tumor-intrinsic PD-L1-NLRP3 inflammasome signaling pathway drives resistance to anti-PD-1 immunotherapy. J Clin Invest 130:2570–2586. https://doi.org/10.1172/JCI133055
40. Bruchard M, Mignot G, Derangère V et al (2013) Chemotherapy-triggered cathepsin B release in myeloid-derived suppressor cells activates the Nlrp3 inflammasome and promotes tumor growth. Nat Med 19:57–64. https://doi.org/10.1038/nm.2999
41. Ghiringhelli F, Apetoh L, Tesniere A et al (2009) Activation of the NLRP3 inflammasome in dendritic cells induces IL-1beta-dependent adaptive immunity against tumors. Nat Med 15:1170–1178. https://doi.org/10.1038/nm.2028
42. Ding Y, Yan YL, Dong YH et al (2022) NLRP3 promotes immune escape by regulating immune checkpoints: a pan-cancer analysis. Int Immunopharmacol 104:108512. https://doi.org/10.1016/j.intimp.2021.108512
43. Kaplanov I, Carmi Y, Kornetsky R et al (2019) Blocking IL-1β reverses the immunosuppression in mouse breast cancer and synergizes with anti-PD-1 for tumor abrogation. Proc Natl Acad Sci USA 116:1361–1369. https://doi.org/10.1073/pnas.1812266115
44. Dixon KO, Tabaka M, Schramm MA et al (2021) TIM-3 restrains anti-tumour immunity by regulating inflammasome activation. Nature 595:101–106. https://doi.org/10.1038/s41586-021-03626-9
45. Qian BZ, Pollard JW (2010) Macrophage diversity enhances tumor progression and metastasis. Cell 141:39–51. https://doi.org/10.1016/j.cell.2010.03.014
46. Vered M, Yarom N, Dayan D (2005) 4NQO oral carcinogenesis: animal models, molecular markers and future expectations. Oral Oncol 41:337–339. https://doi.org/10.1016/j.oraloncology.2004.07.005
47. Vitale-Cross L, Czerninski R, Amornphimoltham P et al (2009) Chemical carcinogenesis models for evaluating molecular-targeted prevention and treatment of oral cancer. Cancer Prev Res (Phila) 2:419–422. https://doi.org/10.1158/1940-6207.CAPR-09-0058
48. Zeng Q, Fu J, Korrer M et al (2018) Caspase-1 from human myeloid derived suppressor cells can promote T-cell independent tumor proliferation. Cancer Immunol Res 6:566–577. https://doi.org/10.1158/2326-6066.CIR-17-0543